



ELSEVIER

Available online at www.sciencedirect.com

ScienceDirect

www.elsevier.com/locate/jes

JES

JOURNAL OF
ENVIRONMENTAL
SCIENCESwww.jesc.ac.cn

Research Article

Suitability of using carbon dioxide as a tracer gas for studying vehicle emission dispersion in a real street canyon

Q1

Yuhan Huang^{1,*}, Helen B. Wang^{2,*}, Hilda M.W. Mak², Mengyuan Chu³, Zhi Ning³, Bruce Organ⁴, Edward F.C. Chan², Chun-Ho Liu⁵, Wai-Chuen Mok⁵, Christof Gromke⁶, Ho Kyong Shon¹, Chengwang Lei⁷, John L. Zhou¹

¹Centre for Green Technology, School of Civil and Environmental Engineering, University of Technology Sydney, NSW, 2007, Australia

²Faculty of Science and Technology, Technological and Higher Education Institute of Hong Kong, Hong Kong, China

³Division of Environment and Sustainability, The Hong Kong University of Science and Technology, Hong Kong, China

⁴Jockey Club Heavy Vehicle Emissions Testing and Research Centre, Vocational Training Council, Hong Kong, China

⁵Department of Mechanical Engineering, The University of Hong Kong, Hong Kong, China

⁶Laboratory of Building and Environmental Aerodynamics, Institute for Water and Environment, Karlsruhe Institute of Technology, Karlsruhe, Germany

⁷Centre for Wind, Waves and Water, School of Civil Engineering, The University of Sydney, NSW, 2006, Australia

ARTICLE INFO

Article history:

Received 30 October 2023

Revised 23 June 2024

Accepted 25 June 2024

Available online xxx

Keywords:

Vehicle emission dispersion

Tracer gas

Carbon dioxide

Urban street canyon

Line emission source

Point emission source

ABSTRACT

High-rise buildings form deep urban street canyons and restrict the dispersion of vehicle emissions, posing severe health risks to the public by aggravating roadside air quality. Field measurements are important for understanding the dispersion process of tailpipe emissions in street canyons, while a major challenge is the lack of a suitable tracer gas. Carbon dioxide (CO₂), which is safe to the public and inexpensive to obtain, can be reliably measured by existing gas analysers. This study investigated the suitability of using CO₂ as a tracer gas for characterising vehicle emission dispersion in a real-world street canyon. The tracer gas was released via a line or point source, whose dispersion was characterised by a sensors network comprising low-cost air quality sensors. The results showed that the CO₂ contained in the exhaust gas of a test vehicle itself had unmeasurable effect at roadsides. Both the line and point sources produced obvious CO₂ level elevations at approximately 30 s after the test vehicle passed by. In addition, for both line and point sources, the CO₂ elevations were much more distinct at the roadside next to tailpipe exit than the opposite side, and were higher at 0.8 m than 1.6 m above the ground. The present study demonstrated that using CO₂ as a tracer gas is feasible for investigating vehicle emission dispersion in real-world

* Corresponding authors.

E-mails: yuhan.huang@uts.edu.au (Y. Huang), beiwang@vtc.edu.hk (H.B. Wang).

<https://doi.org/10.1016/j.jes.2024.06.036>

1001-0742/© 2024 The Research Center for Eco-Environmental Sciences, Chinese Academy of Sciences. Published by Elsevier B.V. This is an open access article under the CC BY license (<http://creativecommons.org/licenses/by/4.0/>)

Please cite this article as: Yuhan Huang, Helen B. Wang, Hilda M.W. Mak et al., Suitability of using carbon dioxide as a tracer gas for studying vehicle emission dispersion in a real street canyon, Journal of Environmental Sciences, <https://doi.org/10.1016/j.jes.2024.06.036>

street canyons. Future studies are needed to improve the gas release rate of the developed tracer gas systems for more reliable measurements and larger street canyons.

© 2024 The Research Center for Eco-Environmental Sciences, Chinese Academy of Sciences. Published by Elsevier B.V.

This is an open access article under the CC BY license (<http://creativecommons.org/licenses/by/4.0/>)

Introduction

1 Ambient air pollution at both street and regional levels re-
2 mains a serious environmental problem in Hong Kong (Cheng
3 et al., 2021; Hossain et al., 2021). The Hedley Environmental
4 Index (2023) estimated that air pollution in Hong Kong caused
5 1329 premature deaths, 1.7 million doctor visits and HK\$15.8
6 billion total economic losses in 2021. Roadside air pollution
7 problem is usually more serious than background air pollu-
8 tion due to the proximity to emission sources (i.e., motor ve-
9 hicles) and the reduced emission dispersion capability when
10 urban street canyons are present (Huang et al., 2021; Pettit
11 et al., 2021; Yang et al., 2020). The Hong Kong air quality moni-
12 toring network data showed that the annual average nitrogen
13 dioxide (NO₂) concentrations measured at roadside stations
14 were much higher (e.g., 45%–210% higher in 2018) than those
15 at background stations (Huang et al., 2020b). Similar roadside
16 air pollution problems were also widely observed in many
17 other cities globally (Casquero-Vera et al., 2019; Grange et al.,
18 2017; Takekawa et al., 2013; Wu et al., 2022). This poses a se-
19 vere health risk to the public, considering that urban streets
20 are important communal places for city inhabitants nowadays
21 (Alexeeff et al., 2018; Huang et al., 2022; Rivas et al., 2019).

22 Developed countries predominantly adopt low develop-
23 ment density and hence are less affected by roadside air
24 pollution aggravated by urban street canyons. However, land
25 scarcity has made tall and dense buildings a typical feature of
26 Hong Kong's cityscape (Kwok et al., 2021; Zheng et al., 2018),
27 leading to the formation of many urban street canyons with
28 high aspect ratios of building height over street width. Insuf-
29 ficient understanding of the pollutant dispersion process lim-
30 its our capability to evaluate the effectiveness of control mea-
31 sures and the implications of city development projects for
32 roadside air quality (Lee, 2019; Li and Zhou, 2019; Zhou and
33 Lin, 2019).

34 Field measurements are essential for understanding the
35 dispersion process of tailpipe emissions in urban street
36 canyons. A proper tracer gas is the key for dispersion exper-
37 iments (Mendes et al., 2015; Simmonds et al., 2021).
38 According to Laporte et al. (2001), an ideal tracer gas should
39 possess a number of characteristics, including: 1) no harm
40 to people, materials or activities in the experimental area, 2)
41 not inflammable, toxic or explosive, 3) no chemical/physical
42 reactions, absorptions or decompositions in the environment,
43 4) similar molecular weight to that of air, 5) no interfer-
44 ence/impacts on the studied process or air movement, 6)
45 absent in air, and 7) amenable to accurate detection at low
46 concentrations. Unfortunately, no tracer gas can fully meet
47 all the above criteria and some additional considerations are
48 necessary when choosing a tracer gas, such as gas cost and
49 measurement equipment (Laporte et al., 2001).

Sulphur hexafluoride (SF₆) is odourless, non-toxic, inert
and exotic to the environment, and can be reliably measured
at very low concentrations (at ppb levels) (Connan et al., 2011;
Guo et al., 2001; Xu et al., 2013). Therefore, SF₆ has been widely
used as a tracer gas for air dispersion studies, in particular in
laboratory wind tunnel investigations. Gromke et al. (2016) in-
vestigated the effect of roadside hedgerows on traffic pollu-
tant dispersion in a reduced scale (1:150) street canyon model
using a line source releasing SF₆ in a wind tunnel. They found
that continuous hedgerows could effectively reduce street-
level pollutant concentrations, especially in the most polluted
centre area of a street canyon. Huang et al. (2020a) measured
the thermal effect on dispersion of rooftop stack emissions
in a step-down street canyon (scale of 1:100) using a point
source emitting SF₆ in a wind tunnel. The results showed that
the thermal effect on the downwind building roof increased
emission dispersion to the upper urban boundary layer and
thus reduced street-level air pollution. Zhang et al. (2022) mea-
sured and simulated the effect of an obstacle on the trans-
port process of a dense gaseous contaminant (represented
by SF₆) in a closed chamber. They revealed three transport
modes (i.e., passive, transitional, and active) around the con-
taminant source, among which the active transport mode had
the highest overall ventilation efficiency. Fu et al. (2022) devel-
oped a fast-response SF₆ measuring system based on a quartz-
enhanced photoacoustic spectroscopy (QEPAS) and evaluated
its performance against a conventional commercial instru-
ment. The results showed that, while both instruments could
obtain similar average concentrations, the QEPAS instrument
successfully captured the rapidly changing SF₆ concentra-
tions, but the conventional commercial instrument did not.

To date, very few studies have been carried out in real-
world street canyons to characterise the dispersion process of
vehicle emissions. SF₆ would not be a suitable tracer gas for
such applications due to the following reasons. Firstly, real-
world dispersion of vehicle emissions is highly dynamic, of-
ten changing within seconds, necessitating rapid measure-
ments to capture the transient variations of tracer gas con-
centrations. However, the prevalent commercial SF₆ measure-
ment instruments usually have long sampling durations and
data acquisition intervals (up to 45 s) (Fu et al., 2022). Secondly,
the density of SF₆ (6.17 kg/m³) is much larger than those of
air (1.23 kg/m³) and vehicle emissions (e.g., 1.87 kg/m³ for CO₂
and 1.14 kg/m³ for CO), which would lead to different disper-
sion characteristics, especially when the flow field is laminar
or of low turbulence, and thus would not represent the dis-
persion of vehicle emissions. Laporte et al. (2001) compared
the performance of two tracer gases, namely SF₆ (6.17 kg/m³)
and N₂O (1.22 kg/m³, practically the same density as that of
air). Their experimental results showed that N₂O tended to
mix and disperse more quickly than SF₆ due to its much lower

101 density. Thirdly, SF₆ is the most potent greenhouse gas whose
 102 global warming potential is 23,500 times of CO₂ (Harrison,
 103 2020; Li et al., 2019). This becomes especially concerning since
 104 field experiments would necessitate a much larger quantity of
 105 gas than wind tunnel experiments. Finally, SF₆ is costly.

106 In contrast, CO₂ is an odourless, inert, non-toxic and in-
 107 expensive gas with a density similar to that of air, whose
 108 measurements can be conducted at a much lower cost and
 109 higher frequency than SF₆. Therefore, CO₂ could be a suitable
 110 tracer gas for representing the dispersion process of vehicle
 111 emissions. The challenge, however, is to develop a CO₂ tracer
 112 gas system (including a measurement sensors network) that
 113 could study the dispersion process of tailpipe emissions in an
 114 urban street canyon in the presence of concurrent CO₂ emis-
 115 sions from vehicles in the study environment. CO₂ was de-
 116 ployed to simulate the dispersion of toxic heavy gases in street
 117 canyons using wind tunnel experiments and CFD modelling
 118 (Tan et al., 2019; 2018). However, to the best of the authors'
 119 knowledge, no experimental studies have used CO₂ as a tracer
 120 gas to investigate the dispersion process of vehicle emissions.

121 Accordingly, this paper aimed to examine the suitability of
 122 using CO₂ as a tracer gas for studying the dispersion process of
 123 tailpipe emissions in a real-world street canyon. A tracer gas
 124 system was developed to release CO₂ gas at a quantity suf-
 125 ficient to reveal the dispersion characteristics of the tailpipe
 126 emissions despite the interference from the CO₂ emissions of
 127 a test vehicle itself. To verify the adequacy of the developed
 128 tracer gas system, a novel test method of combining two emis-
 129 sion measurement techniques, including a portable emission
 130 measurement system (PEMS) and a roadside emission sensor
 131 network (RESN) composed of low-cost small-size air quality
 132 sensors, was developed for characterising the CO₂ dispersion
 133 process, which provided a full picture from tailpipe to road-
 134 side.

1. Materials and methods

1.1. Test site and vehicle

136 Field experiments were carried out on a private road where
 137 the CO₂ emissions were from sources dedicated to the ex-
 138 periments, i.e., a CO₂ line/point source for simulating vehi-
 139 cle emissions on a road and a diesel test vehicle for gener-
 140 ating turbulence as a result of vehicle movement, on top of
 141 a general background CO₂ level (i.e., ~400 ppm in this study)
 142 that was monitored during the experiments. The test site was
 143 a private road on the THEi Tsing Yi Campus (Fig. 1a), which
 144 has a 10-storey building of about 100-m length on one side
 145 and a steep hill several times taller than the building on the
 146 other side. The test vehicle was an IVECO EURO CARGO diesel
 147 medium goods vehicle (Fig. 1b), with a manufacture year of
 148 2018, an engine displacement of 6728 cc, and a gross vehicle
 149 weight of 16 t. A set of PEMS was installed on the test vehicle
 150 to take comprehensive measurements at a frequency of 1 Hz,
 151 including the exhaust flow rate, exhaust temperature, emission
 152 concentration, vehicle speed, air humidity and air tempera-
 153 ture. The exhaust tailpipe was pointing at the left rear wheel
 154 after the installation of the PEMS and the point source tracer
 155 gas system (Fig. 1b).



Fig. 1 – Experimental setup. (a) the test site; (b) the roadside emission sensors and the test vehicle equipped with PEMS.

1.2. Line source experiments

156

157 Fig. 2 shows the setup of the line source experiments. The CO₂
 158 line source was placed on the building side at about 0.3 m from
 159 the RESN. It was a 20-m long steel reinforced polymer hose
 160 with an inner diameter of 1.0 inch (25.4 mm). CO₂ was released
 161 from holes that were 0.5-m equispaced along its length. The
 162 hole diameter was 5.00 mm in the first 10 m and was increased
 163 to 6.35 mm in the second 10 m. Further to this, some holes
 164 were partially blocked by tapes to ensure even release (spa-
 165 tially homogeneous) of the gas along the line source, which
 166 was checked by ambient air sensors at their respective mea-
 167 surement locations. Such checks were performed, and adjust-
 168 ments were made (if required) before each line source mea-
 169 surement series.

170 The line source was supplied by a 180-L liquid gas cylinder
 171 which had a nominal net weight of 175 kg, a gas purity level
 172 of 99.7 % and a maximum pressure of 25 bar. The line source
 173 and CO₂ cylinder were connected by another steel reinforced
 174 polymer hose with a length of 6 m and an inner diameter of 0.5
 175 inch (12.7 mm). A high-flow high-purity Vigour VSR3ELC gas
 176 regulator was fitted to the gas bottle to ensure a constant gas
 177 supply. The gas flow was actuated with a manually controlled
 178 valve at the beginning of each line source test run. Due to the
 179 rapid cooling associated with phase change from liquid to gas
 180 CO₂, the regulator and valves were kept warm by hot air guns
 181 to avoid freezing the regulator or sealing components.

182 The RESN was used to characterise the CO₂ dispersion pro-
 183 cess at both roadsides, which consisted of six pairs of low-cost
 184 small-size air quality sensors. The sensors used in the experi-
 185 ments are HKUST in-house sensors referred to as High Speed
 186 Sensors (HSS). HSS are small size (205 mm × 160 mm × 90 mm)
 187 and light weight (<1.15 kg), include pumps for active sampling,

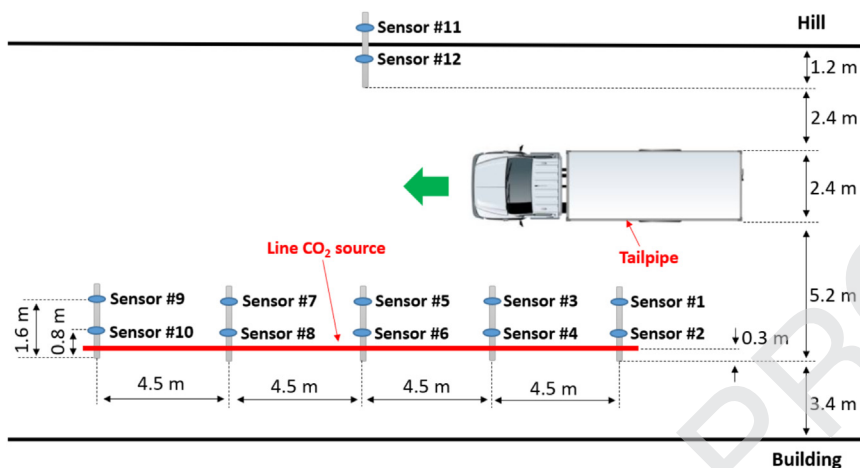


Fig. 2 – Setup of line emission source experiments.

188 and cause negligible obstruction for CO₂ dispersion. The Premier Platinum Infrared High Power Dual Range CO₂ Sensor (Dynament, UK) was used for CO₂ measurements, which operates based on nondispersive infrared (NDIR) method. The sensor can measure a range of CO₂ from 0 to 5% by volume (set as 1% in this study), with a resolution of 10 ppm by volume and a response time of T₅₀ < 10 s. The sensor is temperature compensated over the range of -20 °C to 50 °C. Gas concentrations and system status data were transmitted to a local server for real-time monitoring and stored locally in an SD card for backup. With a built-in pump and a battery, the HSS can operate continuously for more than 12 h. More information about the HSS can be found in our earlier works (Brimblecombe et al., 2021; Chu et al., 2022).

202 All sensors were calibrated at the beginning of the experiments. They sampled CO₂ concentrations at 1 Hz when the line source was switched on and/or the test vehicle passed by. Before experiments began, pilot trials with three pairs of sensors on each roadside were performed, which showed that the sensors on the hill side could not measure any obvious CO₂ changes. Therefore, only one pair of sensors was placed on the hill side and the rest five pairs of sensors were placed on the building side to capture CO₂ variations at a higher spatial resolution. Each pair of sensors was installed on a tripod with a 4.5 m spacing. The sensor heights represented two typical human breathing zones, i.e., 0.8 m for children and 1.6 m for adults (Fig. 2). In addition to the considerations of human breathing zones, the measurements at two different sensor heights are also very useful for developing and calibrating an urban canyon emission dispersion model in future studies.

218 The experiments were conducted under three scenarios (Table 1), including 1) test vehicle only, 2) line source only, and 220 3) test vehicle plus line source. In the test vehicle only scenario, the vehicle drove through the street canyon at three constant speeds of 5, 15 and 30 km/h, which served as the only CO₂ emission source. This was to investigate if the CO₂ gas exhausted from the test vehicle itself would cause any measurable CO₂ elevations at the roadsides in the studied canyon. 226 In the line source only scenario, the line source was switched

227 on for 20 s at two pressures of 24 and 12 bar, which released 228 about 0.073 and 0.061 kg/s of CO₂ gas, respectively. In the test 229 vehicle plus line source scenario, both the line source (24 and 230 12 bar) and test vehicle (5, 15 and 30 km/h) were used. The line 231 source was switched on only when the vehicle passed through 232 the canyon. This was to investigate the CO₂ dispersion process 233 under the influence of turbulence induced by a moving vehicle. 234

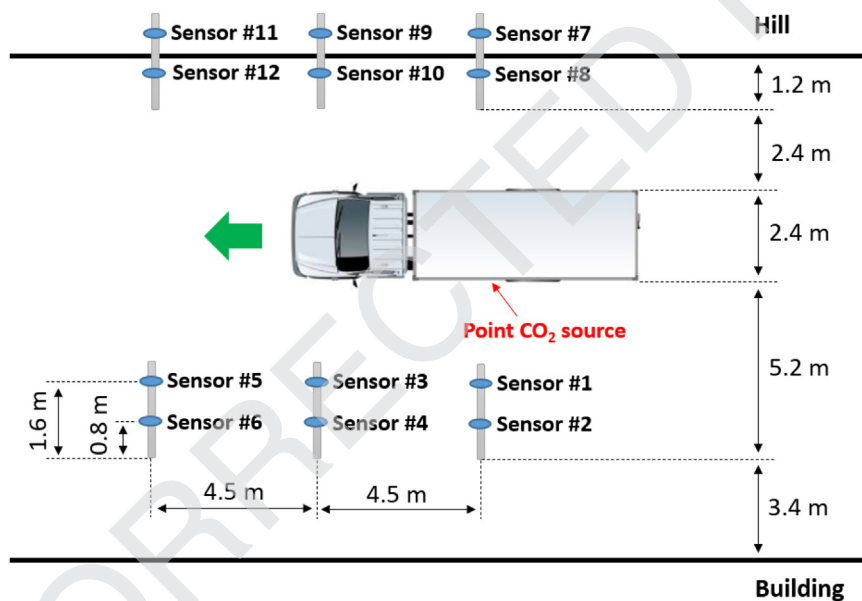
235 Each experimental condition was repeated for at least 236 three times. The RESN sensors recorded the CO₂ concentrations 237 continuously at 1 Hz during the test day. The start and 238 end times of each experiment were logged manually. The ambient 239 conditions of temperature, humidity and wind were also 240 recorded for each experiment. Table 1 also gives the ambi- 241 ent conditions during the experiments. The experiments were 242 performed on a sunny day from 10.30am to 3.00pm. The ambi- 243 ent temperature and humidity were measured by the RESN 244 sensors. The wind speed was measured by a TSI Airflow TA410 245 meter and the wind direction was measured by a compass. 246 The ambient temperature and humidity were relatively stable 247 at around 30 °C and 60 %, respectively, during the whole 248 tests. In comparison, the wind speed was more dynamic be- 249 tween experiments (0.8 – 2.6 m/s, light air to light breeze). 250 However, due to the presence of the steep hill next to the 251 building and the stable prevailing wind direction on the mea- 252 surement day in the Hong Kong region, the wind direction was 253 unchanged during the experiments, which flowed against the 254 vehicle driving direction (Fig. 2).

1.3. Point source experiments

255 Fig. 3 shows the setup of point source experiments. The point 256 source CO₂ tracer gas system was installed inside the con- 257 tainer of the test vehicle, which injected pure CO₂ gas into 258 the exhaust tailpipe. The same type of CO₂ cylinder employed 259 with the line source was used for the point source tests. The 260 gas regulator was also the same, but a remotely actuated gas 261 valve was used to start and stop the gas flow. The actuator 262 used was a Swagelok electric actuator (MS-142DC, 24 V DC) 263

Table 1 – Experimental and ambient conditions.

Experimental conditions		Wind speed (m/s)	Temperature (°C)	Humidity (%)
Scenario 1	Test vehicle only (30 km/h)	2.6	29	64
	Test vehicle only (15 km/h)	1.4	29	66
	Test vehicle only (5 km/h)	0.9	31	61
Scenario 2	Line source only (high rate)	0.8	29	66
	Line source only (low rate)	2.0	34	53
Scenario 3	30 km/h + line source (high rate)	1.9	30	62
	15 km/h + line source (high rate)	2.5	29	63
	5 km/h + line source (high rate)	2.6	29	66
	30 km/h + line source (low rate)	2.3	31	61
	15 km/h + line source (low rate)	1.6	32	58
	5 km/h + line source (low rate)	1.6	33	55

**Fig. 3 – Setup of point emission source experiments.**

264 which was fitted onto the flow control valve. At the start of
 265 a test run, the operator sitting in the cabin of the truck started
 266 the flow from the gas cylinder and stopped the flow after pass-
 267 ing the last gas sensors. A further difference was that a gas
 268 manifold was used to separate the gas flow after the valve
 269 into 4 separate tubes which delivered the gas to equispaced
 270 injection points on the exhaust adapter connected to the ex-
 271 haust pipe of the test vehicle. At the source side, the tailpipe
 272 exhaust flow rates, emission concentrations and temperature
 273 were measured by the PEMS at 1 Hz. At the roadside, three
 274 pairs of air quality sensors were placed at each side of the road
 275 to form a RESN, which measured CO₂ concentrations at 1 Hz
 276 when the test vehicle passed by. Similar to the line source ex-
 277 periments, each pair of sensors was installed on a tripod with
 278 4.5 m spacing, at two typical human breathing heights of 0.8
 279 and 1.6 m above the ground. The experiments were conducted
 280 at 15 km/h driving speed under two conditions, i.e., with and
 281 without the tracer gas system. The ambient wind speeds were
 282 1.3 and 1.2 m/s respectively for the test runs with and without
 283 tracer gas system. The ambient temperatures were relatively
 284 stable at 31.7 °C and 31.3 °C, respectively.

2. Results and discussion

2.1. Line source experiments

Scenario 1. Test vehicle only

285
 286
 287 Fig. 4 shows the variations of CO₂ concentrations measured by
 288 roadside air quality sensors under the test vehicle only sce-
 289 nario (i.e., the CO₂ gas is emitted by the test vehicle only). The
 290 time starts (i.e., 0 s) when the vehicle head passes by the first
 291 pair of sensors (i.e., Sensors #1 and #2 in Fig. 2). The experi-
 292 ments were repeated three times and the plotted curves are
 293 the averaged values of the three tests. To ensure data quality,
 294 calibrations were carried out before and after the experiments.
 295 It was confirmed that all sensors were performing within their
 296 accuracy specifications, except for one which was malfunc-
 297 tioning (i.e., sensor #3 in Fig. 2 and sensor #1 in Fig. 3). The data
 298 from the faulty sensor were omitted in the following analy-
 299 sis and discussion. This data omission would cause little im-
 300 pact on the analysis or conclusions because only one out of 12
 301 sensors was malfunctioning and other adjacent sensors could

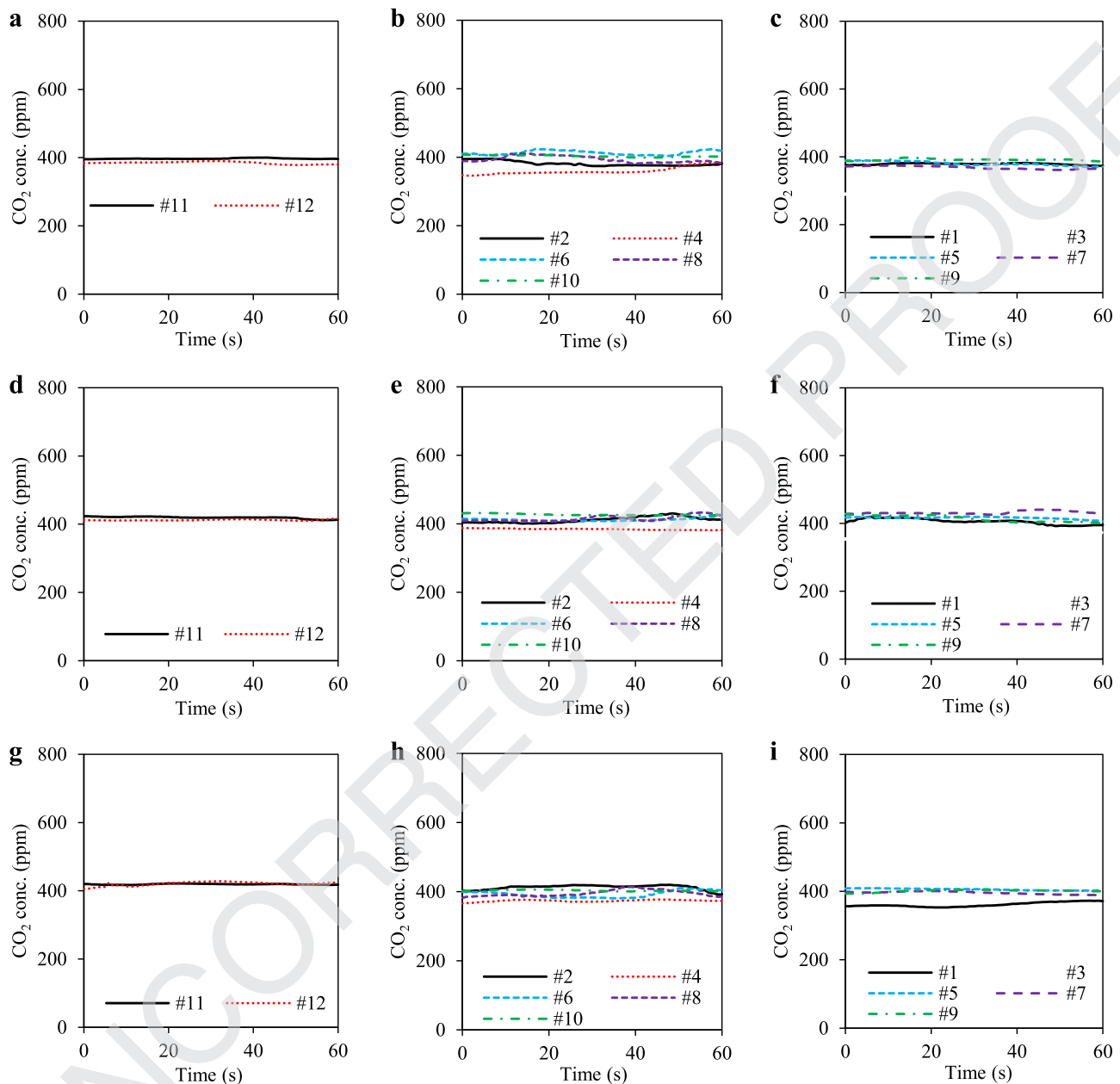


Fig. 4 - Variations of CO₂ concentrations with time measured by roadside air quality sensors under the test vehicle only scenario at various vehicle speeds. (a) 5 km/h - hill side @ 0.8 & 1.6 m; (b) 5 km/h - building side @ 0.8 m; (c) 5 km/h - building side @ 1.6 m; (d) 15 km/h - hill side @ 0.8 & 1.6 m; (e) 15 km/h - building side @ 0.8 m; (f) 15 km/h - building side @ 1.6 m; (g) 30 km/h - hill side @ 0.8 & 1.6 m; (h) 30 km/h - building side @ 0.8 m; (i) 30 km/h - building side @ 1.6 m.

302 compensate the impact. As shown in Fig. 4, there are no obvi-
 303 ous concentration spikes when the test vehicle passes by, at
 304 either the building or the hill side. In general, all the sensors
 305 only measure the background CO₂ concentrations at around
 306 400 ppm. According to the PEMS data, the exhaust mass flow
 307 rates of the test vehicle are 0.070, 0.088 and 0.069 kg/s at 5,
 308 15 and 30 km/h, respectively. The corresponding CO₂ concen-
 309 trations are 2.4%, 4.1% and 6.1%, respectively. Fig. 4 indicates
 310 that the exhaust gas produced by test vehicle itself is too small
 311 to cause any obvious CO₂ elevations at roadsides, and thus
 312 should have insignificant effect on the developed tracer gas
 313 system.

Scenario 2. Line source only

314 Fig. 5 shows the variations of roadside CO₂ concentrations un-
 315 der the line source only scenario (i.e., all CO₂ gas is emitted by
 316 the line source system). The time starts when the line source
 317 is switched on. The experiments were repeated three times
 318 for the high CO₂ release rate condition and four times for the
 319 low CO₂ release rate condition. The plotted curves are the av-
 320 eraged values. Comparing with the test vehicle only scenario
 321 (Fig. 4), Fig. 5 shows obvious CO₂ elevations at the building side
 322 under the line source only scenario due to the much higher
 323 CO₂ release rates (i.e., 0.061–0.073 kg/s pure CO₂ gas from the
 324 line source vs 0.069–0.088 kg/s exhaust gas with 2.4%–6.1%
 325

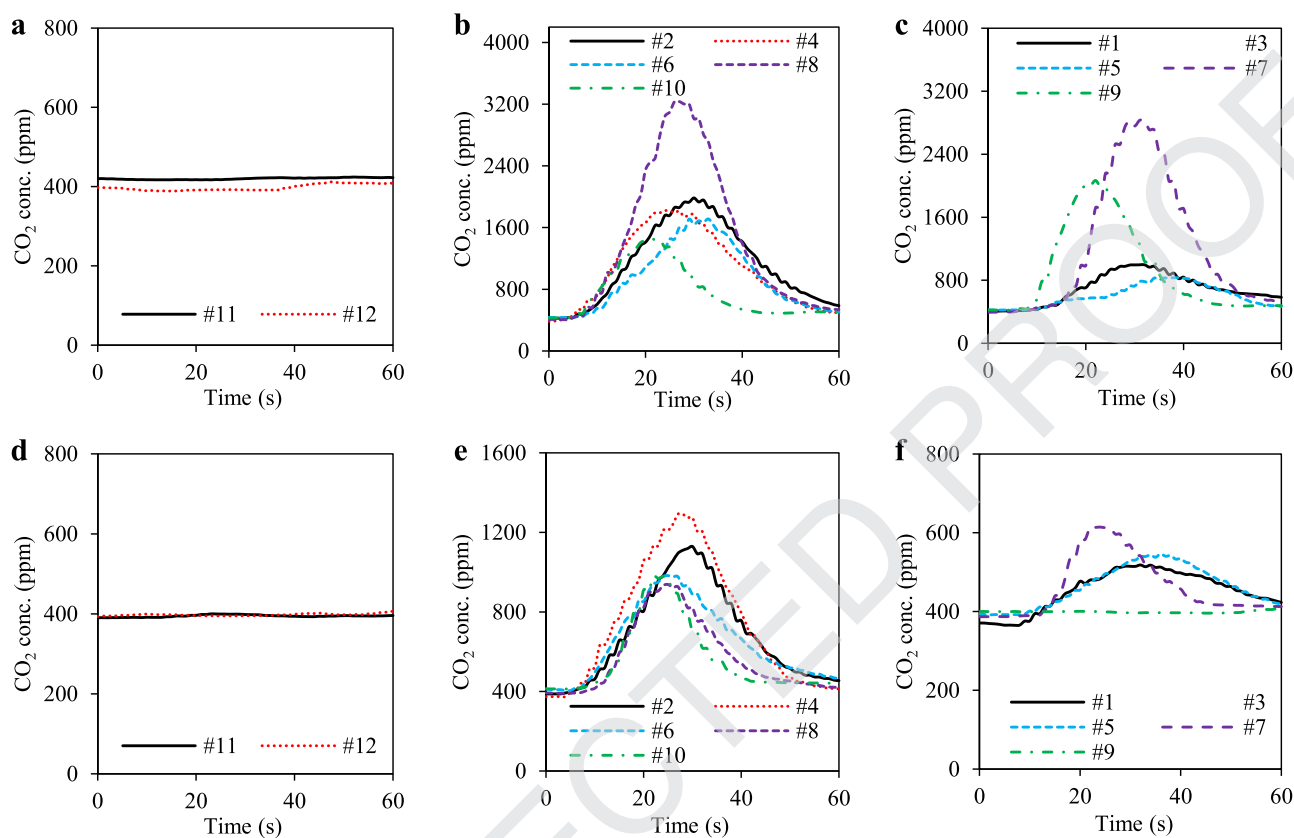


Fig. 5 – Variations of CO₂ concentrations with time measured by roadside air quality sensors under the line source only scenario. (a) High CO₂ release rate - hill side @ 0.8 & 1.6 m; (b) High CO₂ release rate - building side @ 0.8 m; (c) High CO₂ release rate - building side @ 1.6 m; (d) Low CO₂ release rate - hill side @ 0.8 & 1.6 m; (e) Low CO₂ release rate - building side @ 0.8 m; (f) Low CO₂ release rate - building side @ 1.6 m.

CO₂ from the test vehicle). However, the hill side sensors still could not measure any obvious changes under the line source only scenario. The line source was placed next to the building side sensors (0.3 m, Fig. 2) but far from the hill side sensors (10.9 m, Fig. 2), causing very high CO₂ elevations at the building side but no measurable changes at the hill side. For the same reason, the sensors at 0.8 m height always measured higher CO₂ elevations than those at 1.6 m height. These results imply that, using the current CO₂ release rates, the developed line source system would not be suitable for pollutant dispersion experiments in wide street canyons. The system may likely work for two-lane roads with a divider between the lanes, where the line source can be placed. The line source configuration is a better simulation of the emissions from vehicles on a road in real life. Through the measured data, one can figure out the turbulence induced by vehicle movement in the road section under study, so that an urban canyon emission dispersion model can be developed or validated.

It is also noted that three sensors at 1.6 m (i.e., #1 and #5 in Fig. 5a and #9 in Fig. 5b) recorded obviously lower CO₂ concentrations than their adjacent sensors at the same height. This may be caused by two reasons. First, despite rapid developments in recent years, stability remains a key challenge for

low-cost air quality sensors (Castell et al., 2017; Chojer et al., 2020; Kumar et al., 2015; Liu et al., 2020). In this study, pre- and post-calibrations were conducted to confirm that these three sensors were functioning normally. However, the possibility of having gas path leakage in the sensors, which may occur during the transportation or experiments, could not be ruled out. The leakage could cause a lower response in measurements. To address this issue, future studies may deploy more sensors to compensate faulty readings. Second, although these sensors measured relatively low readings in one experiment, they did capture some peaks in other experiments, suggesting that other factors may have caused these unexpected low readings. More specifically, sensors #1 and #9 were placed at the two ends of the canyon and hence may be more vulnerable to changes in ambient wind conditions. Future studies should deploy anemometers to measure the instantaneous wind speeds and directions along with the roadside air quality sensors.

Fig. 5 also shows that all the CO₂ peak concentrations appear at around 30 s after the line source is switched on. Comparing with the high rate condition (0.073 kg/s), although the CO₂ source rate was only slightly reduced in the low rate condition (0.061 kg/s), the measured roadside CO₂ concentration peak was significantly reduced (~2800 ppm @ 1.6 m and

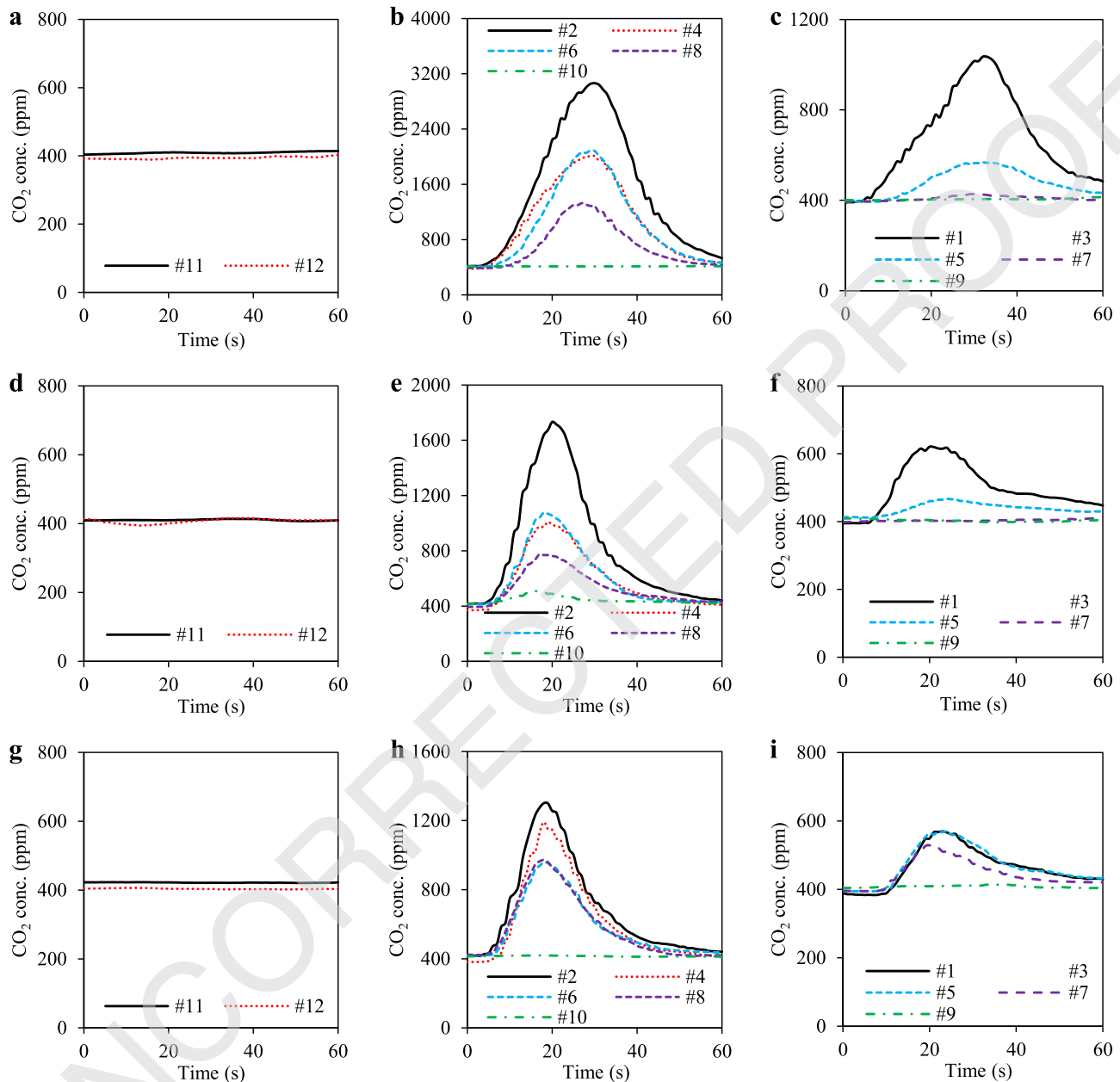


Fig. 6 - Variations of CO₂ concentrations with time measured by roadside air quality sensors under test vehicle plus line source (high CO₂ release rate) scenario at various vehicle speeds. (a) 5 km/h - hill side @ 0.8 & 1.6 m; (b) 5 km/h - building side @ 0.8 m; (c) 5 km/h - building side @ 1.6 m; (d) 15 km/h - hill side @ 0.8 & 1.6 m; (e) 15 km/h - building side @ 0.8 m; (f) 15 km/h - building side @ 1.6 m; (g) 30 km/h - hill side @ 0.8 & 1.6 m; (h) 30 km/h - building side @ 0.8 m; (i) 30 km/h - building side @ 1.6 m.

374 3200 ppm @ 0.8 m under high rate condition vs ~600 ppm @
 375 1.6 m and ~1300 ppm @ 0.8 m under low rate condition). This
 376 is mainly because the ambient wind speed was higher during
 377 the low rate experiments (2.0 m/s) than that during the
 378 high rate experiments (0.8 m/s). A higher wind speed results in
 379 more dilution and facilitates the mixing and dispersion of ex-
 380 haust emissions, leading to lower concentrations at roadsides.
 381 Normalising the roadside CO₂ concentrations by wind speeds
 382 (Gromke and Ruck, 2012) reduces the variations between low
 383 and high rates conditions (see Appendix A Method and Fig.
 384 S1).

Scenario 3. Test vehicle plus line source

385 Figs. 6 and 7 show the effect of vehicle induced turbulence
 386 on the emission dispersion process under high and low line
 387 source rates conditions, respectively. The time starts when the
 388 line source is switched on. All experiments were repeated five
 389 times and the plotted curves were the averaged values. Comparing
 390 with the line source only scenario (Fig. 5), the moving
 391 vehicle facilitates the emission mixing and dispersion pro-
 392 cesses, especially under high driving speed conditions. This
 393 has been clearly demonstrated by the peak CO₂ concentra-
 394 tions and their phases.
 395

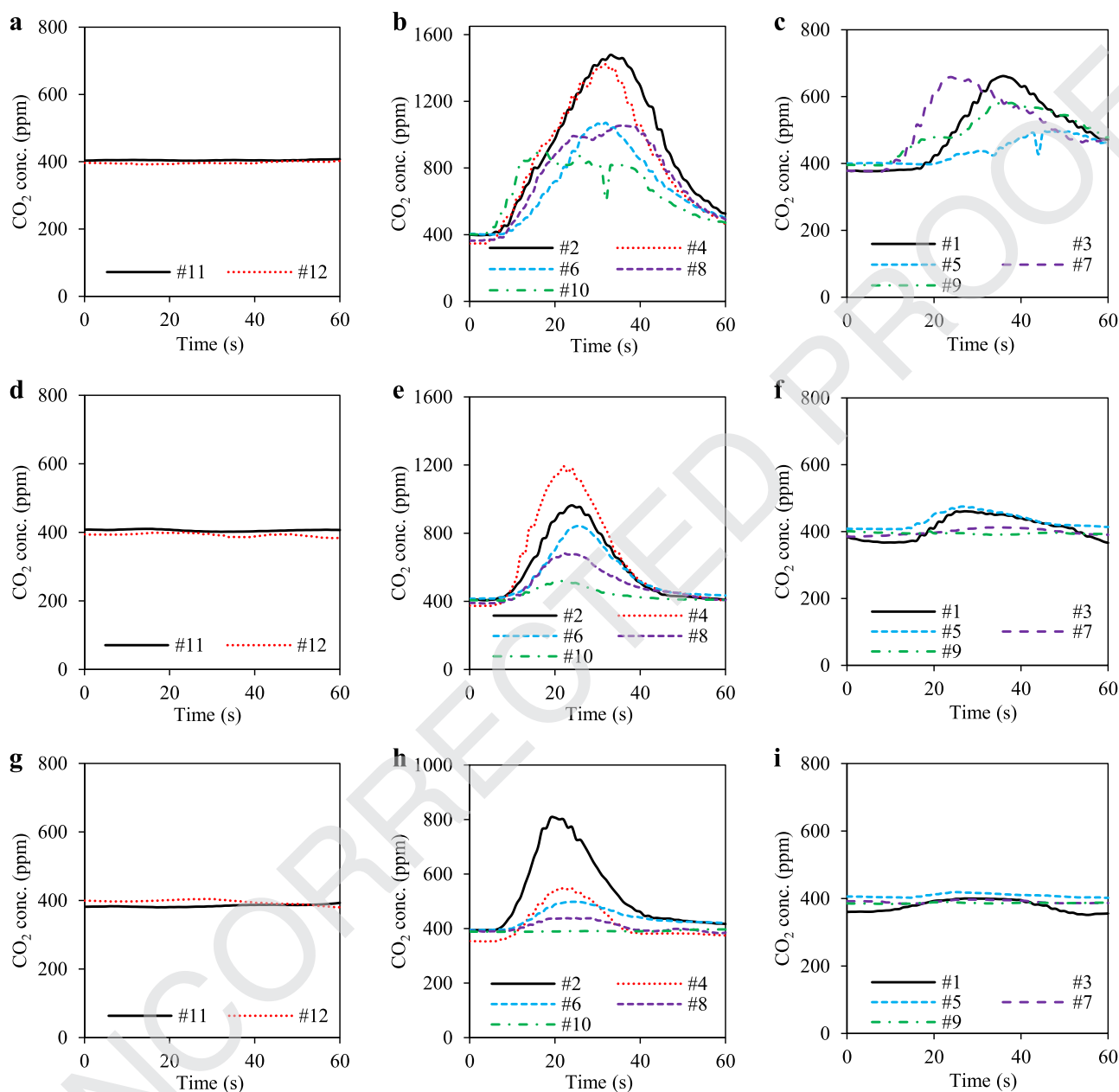


Fig. 7 – Variations of CO₂ concentrations with time measured by roadside air quality sensors under test vehicle plus line source (low CO₂ release rate) scenario at various vehicle speeds. (a) 5 km/h - hill side @ 0.8 & 1.6 m; (b) 5 km/h - building side @ 0.8 m; (c) 5 km/h - building side @ 1.6 m; (d) 15 km/h - hill side @ 0.8 & 1.6 m; (e) 15 km/h - building side @ 0.8 m; (f) 15 km/h - building side @ 1.6 m; (g) 30 km/h - hill side @ 0.8 & 1.6 m; (h) 30 km/h - building side @ 0.8 m; (i) 30 km/h - building side @ 1.6 m.

396 Under the line source only (high rate) condition (Fig. 397 5a), the peak CO₂ concentrations are 3200 ppm @ 0.8 m and 2800 ppm @ 1.6 m, with both appearing at ~ 30 s. They 398 are reduced to 3050 ppm @ 0.8 m and 1000 ppm @ 1.6 m, while the phases are unchanged (~30 s) when the vehicle 399 speed is low at 5 km/h (Fig. 6a). As the vehicle speed increases, the peak concentrations reduce significantly and 400 their phases advance. When the vehicle speed is increased to 401 30 km/h, the peak concentrations are only ~1300 ppm @ 0.8 m and ~600 ppm @ 1.6 m, and their phases advance to ~20 s 402 (Fig. 6c).

In comparison, the effect of vehicle induced turbulence on 407 emission dispersion is less obvious under low line source rate 408 conditions. Under the line source only (low rate) condition (Fig. 409 5b), the peak CO₂ concentrations are ~1300 ppm @ 0.8 m and 410 600 ppm @ 1.6 m, which appear at 30 and 25 s, respectively. At 411 a low vehicle speed of 5 km/h (Fig. 7a), they are even slightly 412 increased to ~1450 ppm @ 0.8 m and 650 ppm @ 1.6 m, and 413 their phases are delayed to ~35 s. At a higher speed of 30 km/h, 414 the peak concentration is reduced to ~800 ppm @ 20 s at the 415 height of 0.8 m, while the CO₂ elevation becomes relatively un- 416 obvious at 1.6 m (Fig. 7c). 417

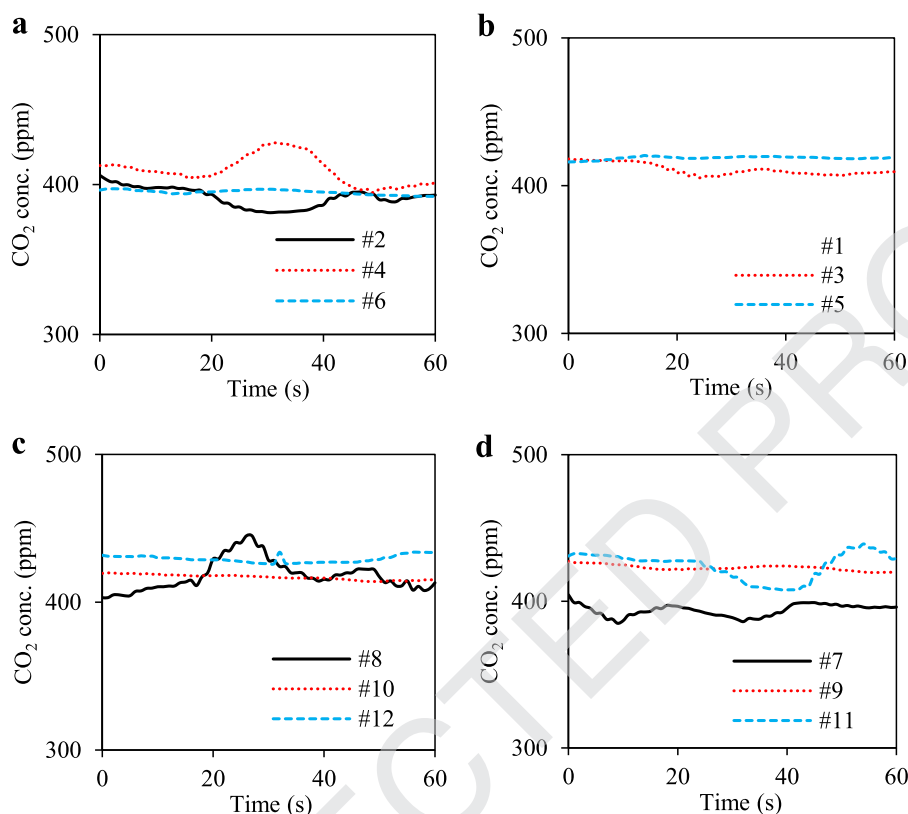


Fig. 8 – Variations of CO₂ concentrations with time measured by individual roadside air quality sensors when point source tracer gas system is off. (a) Building side @ 0.8 m; (b) Building side @ 1.6 m; (c) Hill side @ 0.8 m; (d) Hill side @ 1.6 m.

418 In real-world urban street canyons, vehicle speeds are usually
419 higher than 30 km/h and there are many vehicles passing
420 by continuously, which are expected to greatly enhance
421 the dispersion of vehicle emissions. The results in Figs. 6 and
422 7 imply that the developed line source tracer gas system is
423 suitable for low speed traffic conditions, but requires a higher
424 line source flow rate if it is used for high speed conditions. De-
425 spite the enhancing effect of vehicle induced turbulence on
426 mixing and dispersion of emissions, the hill side sensors still
427 could not measure any CO₂ elevations due to their long distance
428 from the line source. Similar to Fig. 5, we noticed that
429 some sensors (i.e., sensors #7, #9 and #10) captured relatively
430 low readings, probably due to gas path leakage in these sensors
431 and/or changes in ambient winds, as discussed above.

432 2.2. Point source experiments

433 Fig. 8 shows the variations of CO₂ concentrations measured by
434 individual roadside air quality sensors when the point source
435 tracer gas system is off (i.e., all CO₂ gas is emitted by the test
436 vehicle itself). The time starts when the vehicle head passes
437 by the first pair of sensors (i.e., sensors #1 and #2 in Fig. 3).
438 The experiments were repeated three times and the plotted
439 curves are their averaged values. As shown in Fig. 8, generally,
440 there are no obvious concentration spikes when the test vehicle
441 passes by, for both building and hill sides, and at both
442 0.8 and 1.6 m heights. In general, all sensors only measure the
443 background CO₂ concentrations at around 400 ppm. This indi-

444 cates that the exhaust gas from the engine itself would be too
445 small to cause obvious CO₂ elevations at roadsides, and thus
446 should have insignificant effect on the point source tracer gas
447 system.

448 Fig. 9 shows the variations of CO₂ concentrations measured
449 by individual roadside air quality sensors when the point source
450 tracer gas system is on (i.e., CO₂ gas is emitted by both the test
451 vehicle and tracer gas system). The experiments were repeated
452 five times and the plotted curves were the averaged values. In
453 comparison with the tracer gas off condition (Fig. 8), Fig. 9
454 shows obvious CO₂ elevations at the building side at about 35 s
455 after the vehicle passes by. The CO₂ elevations are bigger at the
456 0.8 m than at 1.6 m. However, the sensors at the hill side do
457 not demonstrate any obvious CO₂ elevations.

458 Nevertheless, Fig. 9, as well as Fig. 8, shows significant dif-
459 ferences between individual sensors, which may be caused by
460 signal noises, vibrations, sensor sensitivities and turbulence.
461 Therefore, the CO₂ concentrations measured by the three sensors
462 at the same height (i.e., 0.8 or 1.6 m) and same side (i.e.,
463 building or hill) are averaged, by applying a time delay of 1 s
464 based on 4.5 m sensor spacing and 15 km/h vehicle speed.
465 Such averaging is reasonable for point source experiments (but
466 not for line source experiments) because the three sensors are
467 identical to the emission source except for a 4.5 m spacing.
468

469 Fig. 10 shows the averaged CO₂ concentrations at each sensor
470 height. When the tracer gas system is off, all roadside CO₂
471 concentrations are generally unchanged at the background

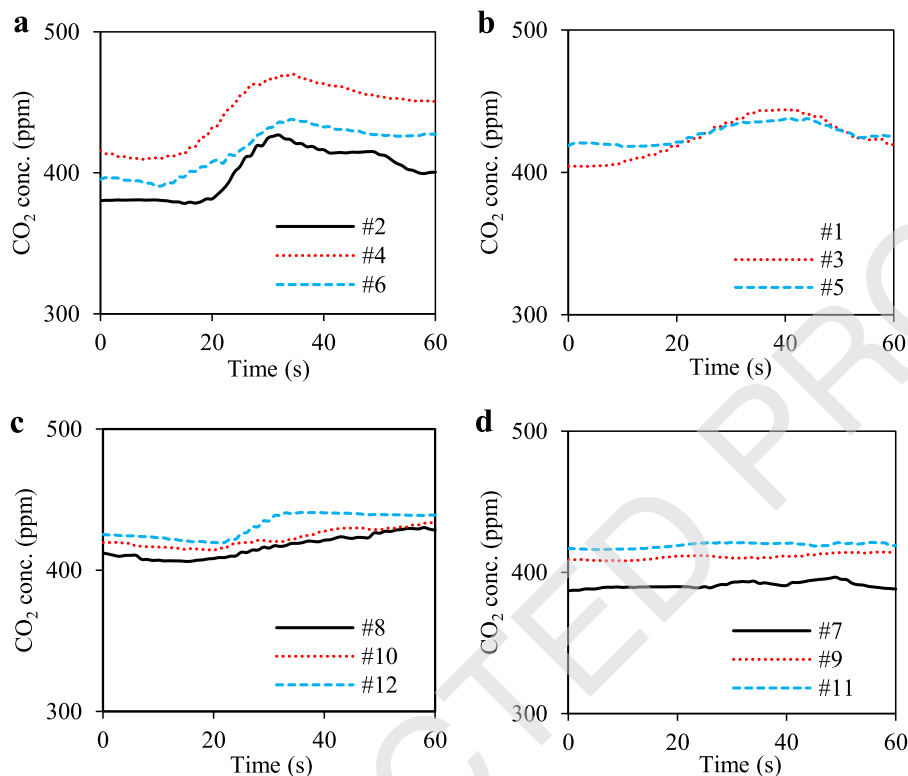


Fig. 9 – Variations of CO₂ concentrations with time measured by individual roadside air quality sensors when the point source tracer gas system is turned on. (a) Building side @ 0.8 m; (b) Building side @ 1.6 m; (c) Hill side @ 0.8 m; (d) Hill side @ 1.6 m.

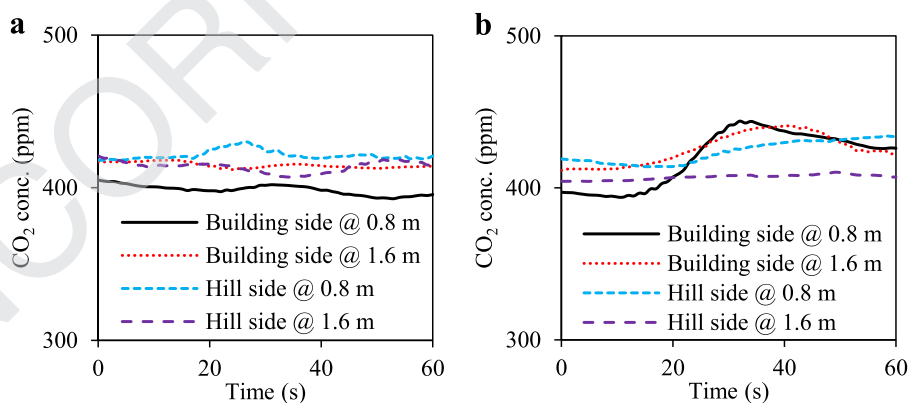


Fig. 10 – Variations of averaged CO₂ concentrations with time. (a) Tracer gas off; (b) Tracer gas on.

472 concentration (i.e., ~400 ppm). When the tracer gas system is
 473 on, roadside air quality sensors at the building side measure
 474 obvious increases in CO₂ concentrations at 30–45 s, while sensors
 475 at the hill side do not measure any noticeable changes.
 476 In addition, CO₂ elevation is more significant at 0.8 m (50 ppm)
 477 than at 1.6 m (40 ppm). This is mainly because the tailpipe exit
 478 is at the building side and is at a height closer to 0.8 m, making
 479 sensors at 0.8 m on the building side the closest to the tailpipe
 480 exit. As a result, exhaust gas has the least dilution when reach-
 481 ing these sensors which consequently record the highest CO₂
 482 increases.

483 Comparing with the line source experiments at the same 483
 484 vehicle speed (i.e., 600–1700 ppm in Fig. 6b and 450–1,200 ppm 484
 485 in Fig. 7b), the CO₂ elevations caused by point source (40– 485
 486 50 ppm in Fig. 10) are much lower. This may be due to two main 486
 487 reasons. Firstly, the point source tracer gas system adopted 487
 488 more connections and valves, leading to much lower CO₂ re- 488
 489 lease rate than the line source system. The PEMS data showed 489
 490 that the point source tracer gas system only released about 490
 491 0.010 kg/s of pure CO₂ gas into the tailpipe of the test vehicle, 491
 492 which was over 80% lower than that of the line source system 492
 493 (i.e., 0.061–0.073 kg/s of pure CO₂ gas). Secondly, the point

494 source was farther to the building side sensors (Fig. 3) than the
495 line source (Fig. 2), leading to greater dispersion when reach-
496 ing the sensors.

3. Conclusions, limitations and recommendations

3.1. Conclusions

498 This study investigated the feasibility of using CO₂ as a tracer
499 gas for characterising the dispersion process of vehicle emis-
500 sions in a real-world street canyon. The experimental data
501 showed unmeasurable CO₂ concentration changes when the
502 test vehicle passed by without the tracer gas system, indicat-
503 ing that the CO₂ gas generated by the test vehicle itself had
504 an insignificant effect. When the tracer gas system was on
505 (for both line and point sources), the roadside air quality sen-
506 sors on the building side measured noticeable CO₂ elevations,
507 while the hill side sensors did not. In addition, the measured
508 CO₂ elevations were larger at 0.8 m than that at 1.6 m.

509 To make CO₂ a suitable tracer gas for studying air pollutant
510 dispersion in an urban street canyon, the benchmark should
511 be whether one can use a practicable amount of the gas (i.e.,
512 CO₂) to adequately characterize air pollutant dispersion. The
513 “practicable amount of the gas” centres on two considerations.
514 One is whether the consumption of the gas is “affordable”,
515 which is to be judged more or less by common sense in terms
516 of cost, safety and health concerns. The other is whether the
517 supply and distribution of the gas can be “conveniently set up
518 in-situ”, particularly at roadside. These are practical consid-
519 erations. To “adequately characterize” the air pollutant disper-
520 sion, the resulting changes in the ambient concentration of
521 the gas at the study location should be of a magnitude suffi-
522 cient for quantifying the dispersion characteristics for disper-
523 sion model development or validation, even though there are
524 other sources of the gas in the measurement locality such as
525 the co-existing vehicles.

526 The experimental data presented in this study demon-
527 strate that the employed CO₂ tracer gas system (both point
528 and line sources) is suitable for characterising emission dis-
529 persion under controlled conditions (i.e., one lane, one vehi-
530 cle), which provides very important data for the development
531 and verification of CFD and Gaussian dispersion models.

3.2. Limitations

533 However, when it comes to real world situation in which there
534 are many vehicles and the line source is placed at road centre
535 (e.g., 1–2 lanes in each direction), the CO₂ changes at roadside
536 may be very small or unmeasurable, unless the line source
537 has a sufficiently high emission rate. This is evidenced by our
538 experimental data since the building side sensors measured
539 high concentrations (0.3 and ~5 m away from line and point
540 sources, respectively), while the hill side sensors measured no
541 CO₂ changes (~10 and ~5 m away from line and point sources,
542 respectively). This is mainly because the current tracer gas
543 system could not release sufficient CO₂ (limited by the valve
544 and condensation). The CO₂ release rate in the present exper-
545 iments was up to 0.073 kg/s for no more than 20 s (i.e., <1.5 kg

of CO₂ per experiment). A bigger tracer gas system will still be
546 affordable, if used for a larger street canyon and placed at road
547 centre.
548

3.3. Recommendations

549 Overall, our field experiments demonstrated that using CO₂
550 as a tracer gas is feasible for investigating vehicle emission
551 dispersion in real-world street canyons. For future field exper-
552 iments, a higher CO₂ release rate is recommended and the de-
553 veloped method is more suitable for small street canyons (e.g.,
554 single- or double-lane streets with low traffic volumes). It is
555 worth noting that this pilot study was preliminary and was
556 not conducted in a typical street canyon as one side of the
557 road was a steep hill. Future studies should be conducted in a
558 real-world urban street canyon to further verify the feasibility
559 of CO₂ as a tracer gas for characterising vehicle emission dis-
560 persion. Furthermore, although experiments were performed
561 in relatively calm days, wind conditions were measured using
562 low-grade devices and hence were paid little attention in the
563 present analysis. Future studies will need to more accurately
564 characterise instantaneous wind speeds and directions to en-
565 able an adequate normalisation of concentration data. Finally,
566 the stability of low-cost sensors remains a challenge. Future
567 studies should adopt more sensors to form a higher resolution
568 sensors network for more reliable statistics and adopt more
569 accurate and reliable sensors if available.
570

Declaration of competing interest

571 The authors declare that they have no known competing finan-
572 cial interests or personal relationships that could have ap-
573 peared to influence the work reported in this paper.

CRediT authorship contribution statement

574 Yuhan Huang: Writing – review & editing, Writing – original
575 draft, Funding acquisition, Formal analysis. Helen B. Wang:
576 Writing – review & editing, Investigation, Funding acquisi-
577 tion. Hilda M.W. Mak: Writing – review & editing, Investiga-
578 tion. Mengyuan Chu: Writing – review & editing, Investiga-
579 tion. Zhi Ning: Writing – review & editing, Funding acquisi-
580 tion. Bruce Organ: Writing – review & editing, Investigation.
581 Edward F.C. Chan: Writing – review & editing, Funding acqui-
582 sition. Chun-Ho Liu: Writing – review & editing, Funding ac-
583 quisition. Wai-Chuen Mok: Writing – review & editing, Fund-
584 ing acquisition. Christof Gromke: Writing – review & editing.
585 Ho Kyong Shon: Writing – review & editing. Chengwang Lei:
586 Writing – review & editing, Supervision. John L. Zhou: Writing
587 – review & editing, Supervision.

Acknowledgements

588 This work was supported by the Environment and Conserva-
589 tion Fund (No. ECF 14/2018) of the Hong Kong SAR Govern-
590 ment, China. Dr Yuhan Huang is a recipient of the ARC Dis-
591 covery Early Career Research Award (DE220100552).
592

Supplementary materials

592 Supplementary material associated with this article can be
593 found, in the online version, at [doi:10.1016/j.jes.2024.06.036](https://doi.org/10.1016/j.jes.2024.06.036).

REFERENCES

- 594 Alexeeff, S.E., Roy, A., Shan, J., Liu, X., Messier, K., Apte, J.S., et al.,
595 2018. High-resolution mapping of traffic related air pollution
596 with Google street view cars and incidence of cardiovascular
597 events within neighborhoods in Oakland. *CA Environ. Health*
598 *17*, 38.
- 599 Brimblecombe, P., Chu, M.-Y., Liu, C.-H., Ning, Z., 2021. NO_x and CO
600 Fluctuations in a Busy Street Canyon. *Environments* *8*, 137.
- 601 Casquero-Vera, J.A., Lyamani, H., Titos, G., Borrás, E., Olmo, F.J.,
602 Alados-Arboledas, L., 2019. Impact of primary NO₂ emissions
603 at different urban sites exceeding the European NO₂ standard
604 limit. *Sci. Total Environ.* *646*, 1117–1125.
- 605 Castell, N., Dauge, F.R., Schneider, P., Vogt, M., Lerner, U.,
606 Fishbain, B., et al., 2017. Can commercial low-cost sensor
607 platforms contribute to air quality monitoring and exposure
608 estimates? *Environ. Int.* *99*, 293–302.
- 609 Cheng, J., Ho, H.C., Webster, C., Su, H., Pan, H., Zheng, H., et al.,
610 2021. Lower-than-standard particulate matter air pollution
611 reduced life expectancy in Hong Kong: a time-series analysis
612 of 8.5 million years of life lost. *Chemosphere* *272*, 129926.
- 613 Chojer, H., Branco, P.T.B.S., Martins, F.G., Alvim-Ferraz, M.C.M.,
614 Sousa, S.I.V., 2020. Development of low-cost indoor air quality
615 monitoring devices: recent advancements. *Sci. Total Environ.*
616 *727*, 138385.
- 617 Chu, M., Brimblecombe, P., Wei, P., Liu, C.-H., Du, X., Sun, Y., et al.,
618 2022. Kerbside NO_x and CO concentrations and emission
619 factors of vehicles on a busy road. *Atmos. Environ.* *271*, 118878.
- 620 Connan, O., Leroy, C., Derkx, F., Maro, D., Hébert, D., Rouspard, P.,
621 et al., 2011. Atmospheric dispersion of an elevated release in a
622 rural environment: comparison between field SF₆ tracer
623 measurements and computations of Briggs and ADMS
624 models. *Atmos. Environ.* *45*, 7174–7183.
- 625 Fu, L., Yang, M., Niu, J., Ren, W., You, R., 2022. Transient tracer gas
626 measurements: development and evaluation of a
627 fast-response SF₆ measuring system based on
628 quartz-enhanced photoacoustic spectroscopy. *Indoor Air* *32*,
629 e12952.
- 630 Grange, S.K., Lewis, A.C., Moller, S.J., Carslaw, D.C., 2017. Lower
631 vehicular primary emissions of NO₂ in Europe than assumed
632 in policy projections. *Nat. Geosci.* *10*, 914–918.
- 633 Gromke, C., Jarmarkattel, N., Ruck, B., 2016. Influence of roadside
634 hedgerows on air quality in urban street canyons. *Atmos.*
635 *Environ.* *139*, 75–86.
- 636 Gromke, C., Ruck, B., 2012. Pollutant concentrations in street
637 canyons of different aspect ratio with avenues of trees for
638 various wind directions. *Boundary-Layer Meteorol* *144*, 41–64.
- 639 Guo, Z., Mosley, R.B., Wasson, S.J., Fortmann, R.C., McBrien, J.A.,
640 2001. Dissociation of Sulfur Hexafluoride Tracer Gas in the
641 Presence of an Indoor Combustion Source. *J. Air Waste Manag.*
642 *Assoc.* *51*, 616–622.
- 643 Harrison, J.J., 2020. New infrared absorption cross sections for the
644 infrared limb sounding of sulfur hexafluoride (SF₆). *J. Quant.*
645 *Spectrosc. Radiat. Transf.* *254*, 107202.
- 646 Hedley Environmental Index, 2023. Historical Data. School of
647 Public Health of The University of Hong Kong Available:
648 <https://hedleyindex.hku.hk/en/historical-data#> Accessed July
649 20, 2023.
- 650 Hossain, M.S., Frey, H.C., Louie, P.K.K., Lau, A.K.H., 2021. Combined
651 effects of increased O₃ and reduced NO₂ concentrations on
short-term air pollution health risks in Hong Kong. *Environ.* *652*
Pollut. *270*, 116280.
- Huang, X.-T., Huang, Y.-D., Xu, N., Luo, Y., Cui, P.-Y., 2020a. Thermal
654 effects on the dispersion of rooftop stack emission in the
655 wake of a tall building within suburban areas by wind-tunnel
656 experiments. *J. Wind Eng. Ind. Aerod.* *205*, 104295.
- 657 Huang, Y., Lee, C.K.C., Yam, Y.-S., Mok, W.-C., Zhou, J.L., Zhuang, Y.,
658 et al., 2022. Rapid detection of high-emitting vehicles by
659 on-road remote sensing technology improves urban air
660 quality. *Sci. Adv.* *8*, eabl7575.
- 661 Huang, Y., Lei, C., Liu, C.-H., Perez, P., Forehead, H., Kong, S., et al.,
662 2021. A review of strategies for mitigating roadside air
663 pollution in urban street canyons. *Environ. Pollut.* *280*, 116971.
- 664 Huang, Y., Mok, W.-c., Yam, Y.-s., Zhou, J.L., Surawski, N.C.,
665 Organ, B., et al., 2020b. Evaluating in-use vehicle emissions
666 using air quality monitoring stations and on-road remote
667 sensing systems. *Sci. Total Environ.* *740*, 139868.
- 668 Kumar, P., Morawska, L., Martani, C., Biskos, G., Neophytou, M., Di
669 Sabatino, S., et al., 2015. The rise of low-cost sensing for
670 managing air pollution in cities. *Environ. Int.* *75*, 199–205.
- 671 Kwok, Y.T., Schoetter, R., de Munck, C., Lau, K.K.-L., Wong, M.S.,
672 Ng, E., 2021. High-resolution mesoscale simulation of the
673 microclimatic effects of urban development in the past,
674 present, and future Hong Kong. *Urban Clim* *37*, 100850.
- 675 Laporthe, S., Virgone, J., Castanet, S., 2001. A comparative study
676 of two tracer gases: SF₆ and N₂O. *Build. Environ.*
677 *36*, 313–320.
- 678 Lee, C., 2019. Impacts of urban form on air quality: emissions on
679 the road and concentrations in the US metropolitan areas. *J.*
680 *Environ. Manage.* *246*, 192–202.
- 681 Li, F., Zhou, T., 2019. Effects of urban form on air quality in China:
682 an analysis based on the spatial autoregressive model. *Cities*
683 *89*, 130–140.
- 684 Li, Y., Zhang, X., Zhang, J., Xiao, S., Xie, B., Chen, D., et al., 2019.
685 Assessment on the toxicity and application risk of C₄F₇N: a
686 new SF₆ alternative gas. *J. Hazard. Mater.* *368*, 653–660.
- 687 Liu, X., Jayaratne, R., Thai, P., Kuhn, T., Zing, I., Christensen, B.,
688 et al., 2020. Low-cost sensors as an alternative for long-term
689 air quality monitoring. *Environ. Res.* *185*, 109438.
- 690 Mendes, L.B., Edouard, N., Ogink, N.W.M., van Dooren, H.J.C.,
691 Tinôco, I.d.F.F., Mosquera, J., 2015. Spatial variability of mixing
692 ratios of ammonia and tracer gases in a naturally ventilated
693 dairy cow barn. *Biosyst. Eng.* *129*, 360–369.
- 694 Pettit, T., Torpy, F.R., Surawski, N.C., Fleck, R., Irga, P.J., 2021.
695 Effective reduction of roadside air pollution with botanical
696 biofiltration. *J. Hazard. Mater.* *414*, 125566.
- 697 Rivas, E., Santiago, J.L., Lechón, Y., Martín, F., Ariño, A., Pons, J.J.,
698 et al., 2019. CFD modelling of air quality in Pamplona City
699 (Spain): assessment, stations spatial representativeness and
700 health impacts valuation. *Sci. Total Environ.* *649*, 1362–1380.
- 701 Simmonds, P.G., Palmer, P.I., Rigby, M., McCulloch, A., O'Doherty, S.,
702 Manning, A.J., 2021. Tracers for evaluating computational
703 models of atmospheric transport and oxidation at regional to
704 global scales. *Atmos. Environ.* *246*, 118074.
- 705 Takekawa, H., Chatani, S., Ito, A., 2013. A new approach for
706 estimation of the effect of NO_x emission reduction on
707 roadside NO₂ concentration in Tokyo. *Atmos. Environ.* *68*,
708 92–102.
- 709 Tan, W., Li, C., Wang, K., Zhu, G., Liu, L., 2019. Geometric effect of
710 buildings on the dispersion of carbon dioxide cloud in
711 idealized urban street canyons. *Process Saf. Environ. Prot.* *122*,
712 271–280.
- 713 Tan, W., Li, C., Wang, K., Zhu, G., Wang, Y., Liu, L., 2018. Dispersion
714 of carbon dioxide plume in street canyons. *Process Saf.*
715 *Environ. Prot.* *116*, 235–242.
- 716 Wu, X., Vu, T.V., Harrison, R.M., Yan, J., Hu, X., Cui, Y., et al., 2022.
717 Long-term characterization of roadside air pollutants in urban
718 Beijing and associated public health implications. *Environ.*
719 *Res.* *212*, 113277.

- 721 Xu, G., Luxbacher, K.D., Ragab, S., Schafrik, S., 2013. Development
722 of a remote analysis method for underground ventilation
723 systems using tracer gas and CFD in a simplified laboratory
724 apparatus. *Tunn. Undergr. Space Technol.* 33, 1–11.
- 725 Yang, J., Shi, B., Zheng, Y., Shi, Y., Xia, G., 2020. Urban form and air
726 pollution disperse: key indexes and mitigation strategies.
727 *Sustain. Cities Soc.* 57, 101955.
- 728 Zhang, Q., Zhang, X., Ye, W., Zhi, C., Huang, Y., Gao, J., 2022.
729 Transport characteristics of dense gaseous contaminants in a
large space in the presence of obstacles. *Build. Environ.* 207, 730
108411. 731
- Zheng, Y., Ren, C., Xu, Y., Wang, R., Ho, J., Lau, K., et al., 2018. 732
GIS-based mapping of Local Climate Zone in the high-density 733
city of Hong Kong. *Urban Clim* 24, 419–448. 734
- Zhou, S., Lin, R., 2019. Spatial-temporal heterogeneity of air 735
pollution: the relationship between built environment and 736
on-road PM_{2.5} at micro scale. *Transp. Res. Part D* 76, 305–322. 737
738